

ChemComm

Accepted Manuscript



This is an *Accepted Manuscript*, which has been through the Royal Society of Chemistry peer review process and has been accepted for publication.

Accepted Manuscripts are published online shortly after acceptance, before technical editing, formatting and proof reading. Using this free service, authors can make their results available to the community, in citable form, before we publish the edited article. We will replace this *Accepted Manuscript* with the edited and formatted *Advance Article* as soon as it is available.

You can find more information about *Accepted Manuscripts* in the [Information for Authors](#).

Please note that technical editing may introduce minor changes to the text and/or graphics, which may alter content. The journal's standard [Terms & Conditions](#) and the [Ethical guidelines](#) still apply. In no event shall the Royal Society of Chemistry be held responsible for any errors or omissions in this *Accepted Manuscript* or any consequences arising from the use of any information it contains.

COMMUNICATION

Multicomponent dipeptide hydrogels as extracellular matrix-mimetic scaffolds for cell culture applications

Cite this: DOI: 10.1039/x0xx00000x

Wathsala Liyanage,^a Kanika Vats,^b Annada Rajbhandary,^a Danielle S. W. Benoit,^{b,d} and Bradley L. Nilsson^{a*}

Received 00th January 2012,

Accepted 00th January 2012

DOI: 10.1039/x0xx00000x

Fmoc-3F-Phe-Arg-NH₂ and Fmoc-3F-Phe-Asp-OH dipeptides undergo coassembly to form two-component nanofibril hydrogels. These hydrogels support the viability and growth of NIH 3T3 fibroblast cells. The supramolecular display of Arg and Asp at the nanofibril surface effectively mimics the integrin-binding RGD peptide of fibronectin, without covalent connection between the Arg and Asp functionality.

Self-assembled supramolecular hydrogel materials are promising scaffolds for tissue engineering.¹⁻¹² Supramolecular hydrogels designed as mimetics of extracellular matrix (ECM) often display integrin binding domains such as the fibronectin-derived Arg-Gly-Asp (RGD) peptide,¹³⁻¹⁵ which promotes cell adhesion, migration, and differentiation.^{16,17} Self-assembled peptide-based hydrogels, including Fmoc-PhePhe/Fmoc-RGD,^{18,19} Fmoc-RGD,²⁰ and (RADA)₄²¹ (in which the RAD motif approximates RGD) have been exploited as materials that support cell culture applications with varying degrees of success. In each of these cases, the resulting materials explicitly incorporate the RGD peptide at an exposed surface of the fibrils that constitute the hydrogel network. Herein, we explore supramolecular hydrogels that do not explicitly contain the RGD peptide, but instead display Arg and Asp separately on supramolecular fibrils in an orientation that facilitates functional mimicry of fibronectin for the promotion of cell growth. Importantly, no covalent connection between the Arg and Asp motifs is incorporated in these materials.

Herein, we report that Fmoc-3F-Phe-Asp-OH (**1**) and Fmoc-3F-Phe-Arg-NH₂ (**2**) dipeptides (Figure 1A) undergo coassembly mediated by aromatic, hydrophobic, and Coulombic interactions to form two-component nanofibrils²² that elicit gelation of water. These hydrogels possess the requisite mechanical and biochemical properties to support the attachment and growth of cells in culture. We have previously exploited Fmoc-Phe derivatives to form supramolecular hydrogels,^{7, 23-27} and we reasoned that appending Arg and Asp to the Fmoc-3F-Phe assembly motif (which we have previously found to exhibit ideal assembly and hydrogelation properties)²⁷ would provide hydrogels that may functionally exhibit integrin-binding properties based on the relative orientation of the Arg and Asp groups in the context of the assembled fibrils. In addition to the biochemical functionality of Arg and Asp display, we also hypothesized that the complementary charges of these amino acids would facilitate effective coassembly to form the desired two-component fibrils.²²

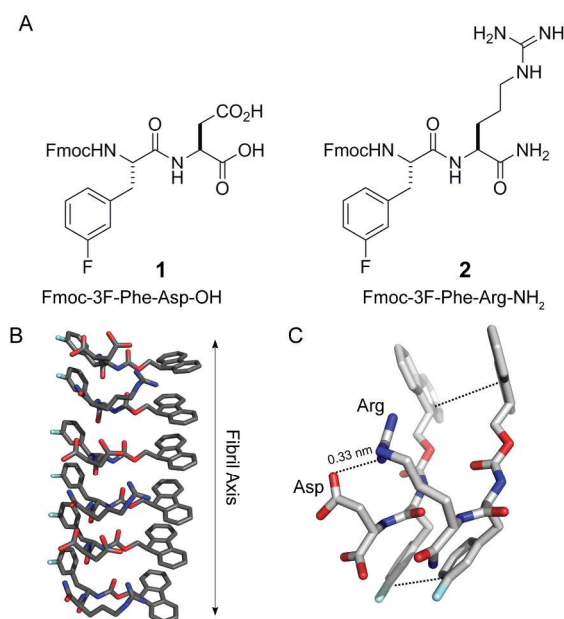


Figure 1. A. Structures of Fmoc-3F-Phe-Asp-OH (**1**) and Fmoc-3F-Phe-Arg-NH₂ (**2**). B. Proposed packing architecture of **1** and **2** in co-assembled fibrils. C. Proposed packing of a dimeric pair of **1** and **2** in the context of coassembled fibrils indicates the possible relative orientation of Arg and Asp in relation to the Fmoc-3F-Phe assembly motif.

Hydrogelation was found to readily occur for most of the mixtures of **1** and **2** that were tested. Coassembly and hydrogelation was initiated by dilution of DMSO stock solutions of **1** and **2** in varying ratios (ratios of **2**:**1** tested were 1:1, 3:2, 7:3, 4:1, 9:1) into water (9.8 mM concentration of total dipeptide in 4% DMSO/H₂O, v/v). Upon dilution, the mixtures formed an opaque suspension that became optically transparent, self-supporting hydrogels in minutes (Table S1, ESI). The self-assembly propensity of each dipeptide was also assessed. The dilution of Fmoc-3F-Phe-Arg-NH₂ from DMSO into water 9.8 mM resulted in the formation of a transparent solution that showed no evidence of gelation, while Fmoc-3F-Phe-Asp-OH spontaneously self-assembles and forms a weak, opaque hydrogel upon dilution into water. The ratios of **2**:**1** in the assembled fibrils

that comprise the hydrogel network were assessed by sedimentation of the assembled hydrogels after mechanically induced precipitation of the fibrils (see ESI for protocols). The sedimented fibrils were disassembled by dissolution in DMSO and concentrations Fmoc-3F-Phe-Asp-OH and Fmoc-3F-Phe-Arg-NH₂ were determined by HPLC analysis (Figure S1, Table S2). The 1:1, 3:2, and 7:3 hydrogels had ratios of **2**:**1** near 1:1 while gels with higher ratios of Arg were found to have higher concentrations of **2** in the resulting fiber networks.

The morphology of the assembled fibrils that define the hydrogel networks was characterized by transmission electron microscopy (TEM). These materials self- or coassemble into nanotape fibrils with diameters 10–21 nm (Figure 2, Figure S2 in ESI). The self-assembled **1** hydrogel consists of twisted nanotapes 21 ± 2 nm in diameter. The 1:1 and 3:2 (**2**:**1**) mixtures coassemble into abundant fibrils that have more narrow and uniform widths of 10 ± 1 nm (Figure 2A, B; Figure S2). These mixtures also contain fibril bundles composed of twisted pairs of narrower fibrils that range from ~14–20 nm in width. The 7:3, 4:1, and 9:1 mixtures (**2**:**1**) are composed of similar narrow twisted tapes with mean widths of 14 ± 2, 11 ± 2, 16 ± 2 nm respectively (Figure S2). Solutions of **2** alone showed no evidence of fibrils, indicating that at low ionic strength this monomer fails to self-assemble into fibrillar structures. Under these assembly conditions, Arg is positively charged and Asp is partially negatively charged, which is consistent with charge repulsion accounting for these observations.

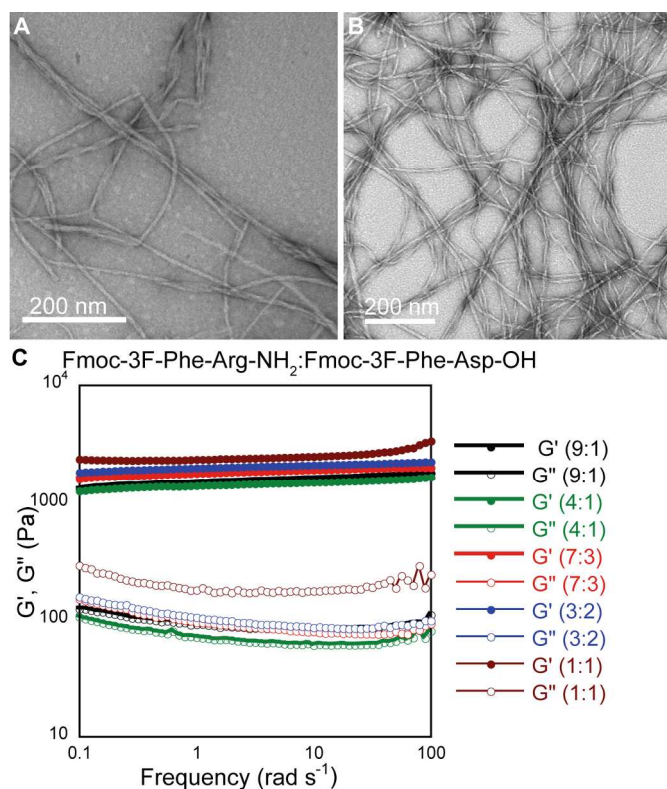


Figure 2. A. TEM image of a 1:1 coassembled mixture of **2**:**1** (9.8 mM total dipeptide). B. TEM image of a 3:2 coassembled mixture of **2**:**1** (9.8 mM total peptide). C. Oscillatory rheology frequency sweep of **2**:**1** coassembled hydrogels (9.8 mM total peptide) (1:1, brown; 3:2, blue; 7:3, red; 4:1, green; 9:1, black).

The electronic structures of the hydrogel assemblies were characterized by circular dichroism (CD) spectroscopy (Figure S3,

ESI). Each hydrogel (9.8 mM total dipeptide) showed characteristic absorptions from 200–220 nm, consistent with $n\text{-}\pi^*$ transitions from self-association of the phenyl side chain groups of Fmoc-3F-Phe.²⁷ A second characteristic absorption was seen from 270–310 nm, indicative of $\pi\text{-}\pi^*$ transitions between offset face-to-face stacked Fmoc groups. These CD spectra are similar to previously reported spectra for hydrogels of self- or coassembled Fmoc-Phe derivatives and are consistent with the proposed dipeptide packing architecture depicted in Figure 1B.^{23–27} At higher ratios of **2** in the **2**:**1** coassembled mixtures (7:3, 4:1, 9:1), the observed CD signal intensity decreased. This is potentially due to lower incorporation of dipeptide **2** into the fibrils as indicated by the previously discussed fibril sedimentation analysis (Figure S1, Table S2).

This CD data is consistent with the proposed packing model shown in Figures 1B and 1C. However, this data cannot be offered as definitive proof of the proposed fibril structure. While CD data is provided in order to qualitatively compare the electronic and chiral nature of the hydrogel fibril network to that of previously reported Fmoc-Phe-derived hydrogels, it cannot be used to define the structure at high resolution. In the absence of data obtained from higher resolution, but challenging solid state NMR experiments, it should be stressed that the structural details of the hydrogel network are not understood. In the following sections, we present functional data regarding the interface of the hydrogel network with cells. This data also generally supports co-presentation of Arg and Asp at the fibril surface similar to the proposed structures in Figure 1.

The rheological viscoelasticity of each of the hydrogels was characterized to ensure that the resulting gels would be adequate for cell culture applications (Table S1). The rheological properties of hydrogels that mimic native ECM play a key role in regulating cell functions.^{7, 9} Hydrogels typically have storage moduli (G') that exceed loss moduli (G'') by an order of magnitude and a minimum G' of approximately 100 Pa to enable suspension of cells.^{9, 28, 29} The viscoelasticity of dipeptide hydrogels was measured using dynamic frequency sweep experiments (Figure 2C) (0–100 rad s⁻¹ at 0.2% strain, which falls into the linear viscoelastic region as determined by prior strain sweeps; a representative strain sweep is shown in Figure S4). The observed storage modulus (G') and loss modulus (G'') values of the hydrogels (Table S1) were essentially independent of frequency. The G' and G'' of the 1:1 mixture were 2481 ± 236 Pa and 197 ± 30 Pa, respectively, and the G' and G'' of the 3:2 mixture was 2029 ± 114 Pa and 102 ± 20 Pa. Both mixtures show excellent solvolytic stability with G' exceeding G'' by an order of magnitude. The Arg-rich co-fibrils (7:3, 4:1 and 9:1 mixtures) displayed weaker viscoelasticity (Table S1, $G' \sim 1400\text{--}1800$ Pa, $G'' \sim 70\text{--}95$ Pa) compared to the 1:1 and 3:2 coassembly mixtures, presumably due to lower incorporation of **2** into fibrils at these ratios (Table S2).

Prior to assessment of these materials as scaffolds for cell culture applications, we also characterized the structural integrity of these gels when exposed to cell culture media. The hydrogels are formed using an organic co-solvent (DMSO) in unbuffered water. After formation of the gels, they were perfused with cell culture media (DMEM supplemented with fetal bovine serum, see ESI for details) to remove organic co-solvent. Media was added to the top of the resulting gels and allowed to stand for 24 hours, after which the media was exchanged. After several washes with cell culture media, the 1:1 and 3:2 (**2**:**1**) coassembled gels displayed excellent stability, with no degradation of gel integrity over time (Figure S5, ESI). In contrast, 7:3, 4:1 and 9:1 (**2**:**1**) mixtures exhibited loss of mechanical integrity after 2–3 days of exposure to buffered media.

The utility of these hydrogels for cell culture applications was then evaluated. Mouse embryonic fibroblast cells (NIH 3T3) were seeded onto the surface (50,000 cells/cm²) of each coassembled hydrogel. As a control, cells were also grown in standard tissue

culture plates (see ESI for details). Within 24 h of cell seeding of hydrogels, cell adhesion was observed with cells adopting spindle/polyhedral shapes (Figure 3, Figures S6–S8). Cells were well spread on the surfaces with cellular extensions. LIVE/DEAD staining of cells were performed 24, 72, and 96 h after seeding. Stable hydrogels composed of 1:1 and 3:2 ratios of **2:1** show 2×10^6 cells/cm² and 1×10^6 cells/cm² cell density after 5 days; cell density and morphology on these materials was indistinguishable from the control tissue culture surface (Figure 3, Figure S10). Hydrogels with 7:3, 4:1, and 9:1 ratios of **2:1** significantly degraded upon exposure to cell culture media, leading to decreased cell attachment within 48 h. In addition, cells on these higher-Arg materials displayed spherical morphologies indicative of poor cell attachment (Figure S10A–D). Thus, hydrogels with nearly equimolar ratios of **2:1** (1:1, 3:2) are much more effective fibronectin-mimetic materials, as would be expected based on the ratios of Arg to Asp approximating the 1:1 display of RGD.

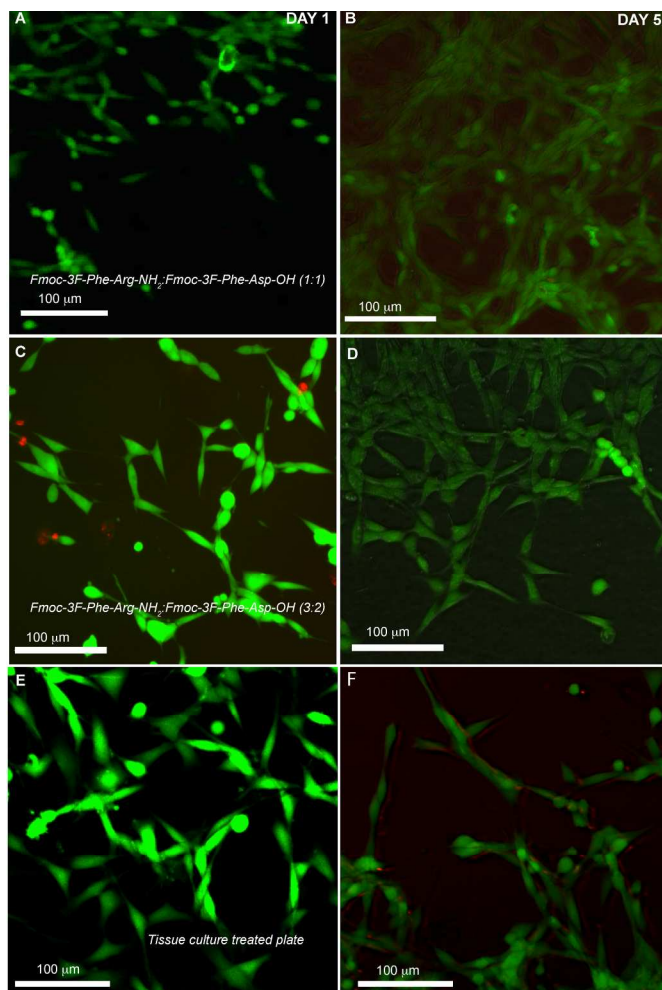


Figure 3. Confocal microscopy images of NIH 3T3 cells 1 and 5 days after cell seeding on 1:1 (**2:1**) hydrogels (A and B, 1 and 5 days respectively), 3:2 (**2:1**) hydrogels (C and D, 1 and 5 days respectively), treated tissue culture plates (E and F, 1 and 5 days respectively). Images are overlays of bright field, and live/dead stained images (live cells are green, dead cells are red).

Scanning electron microscopy (SEM) confirmed that cells seeded on the dipeptide nanofibrous scaffolds adopted typical morphology of attached fibroblasts with adhesive contacts with the gel surface (Figure 4, Figure S11). These observations clearly

indicate that these ionic-complementary hydrogels promote cell-matrix interactions leading to cell adhesion and spreading as well as long-term viability and proliferation. No migration of cells was observed into the hydrogels. Rather, the 3T3 fibroblasts remain at the surfaces of the hydrogels and grow to confluence. After 72–96 h of incubation, the 1:1, 3:2 (**2:1**) coassembled gels show dense fibroblast monolayers evenly spread on the surface of the hydrogel; tight junctions between cells create a uniform tissue-like arrangement (Figures S9 and S11). Clearly, the **2:1** hydrogels containing 1:1 and 3:2 ratios of the constituent dipeptides most favorably exhibit ECM-like behavior compared to more arginine rich coassembly mixtures (7:3, 4:1, and 9:1).

The mechanism of cell adhesion to the hydrogels was examined to determine if the gels exhibit fibronectin RGD-like binding to cellular integrins. Integrin-blocking antibodies were used to conduct these cell adhesion analyses (Figure S12).^{30–33} Untreated cells with (no integrin blocking) and blocked anti- $\alpha 5$ and - $\beta 1$ integrins adhere to the 1:1 gels, while the cells with blocked αv and $\beta 3$ integrins failed to adhere to the Arg/Asp coassembled nanofiber surfaces. This study suggests that integrin $\alpha \beta 3$ is responsible for cell adhesion to the Arg/Asp coassembled gels, consistent with many RGD-functionalized materials.^{30–33} Thus, these hydrogels exhibit fibronectin-mimetic properties by the noncovalent display of Arg and Asp at the nanofiber surface.

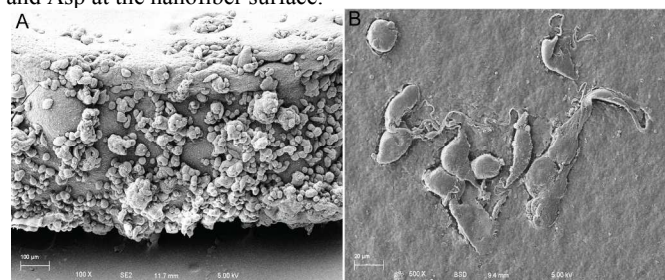


Figure 4. SEM micrographs of interaction between NIH 3T3 fibroblast cells and Fmoc-3F-Phe-Arg:Fmoc-3F-Phe-Asp (1:1) coassembled hydrogels after 2 days. A. 100 \times magnification; B. 500 \times magnification.

In conclusion, herein we have reported that Fmoc-3F-Phe-Arg-NH₂ and Fmoc-3F-Phe-Asp-OH dipeptides undergo coassembly mediated by aromatic, hydrophobic, and Coulombic interactions to form two-component nanofibril hydrogels in water. These hydrogels possess the requisite mechanical and biochemical properties to support the viability and growth of NIH 3T3 fibroblast cells. Fibroblasts cultured on the surface of these gels are viable for longer than five days and continue to proliferate. Cell adhesion at the gel surface is facilitated by the display of Arg and Asp on network-forming fibrils. These studies demonstrate that noncovalent supramolecular display of Arg and Asp provides materials that can effectively mimic the cell adhesive functions of the fibronectin RGD peptide, without covalent connection between the Arg and Asp amino acids. Multicomponent coassembled hydrogel materials that elicit RGD-like responses in cell culture applications expands the possibilities in the design of novel materials for tissue engineering.

The National Science Foundation (DMR-1148836 to BLN and DMR-1206219 to DSWB) and the National Institutes of Health (R01AR064200, R01DE022949, and P30AI078498 to DSWB) supported this research. We gratefully acknowledge Karen Bentley (URMC Electron Microscopy Research Core) for her assistance with TEM and SEM imaging and Dr. Scott Kennedy for assistance with CD experiments.

Notes and references

^aDepartment of Chemistry, University of Rochester, Rochester, NY 14627-0216, USA.

^bDepartment of Biomedical Engineering, University of Rochester, Rochester, NY 14627-0168, USA.

^cDepartment of Chemical Engineering, University of Rochester, Rochester, NY 14627-0166, USA.

^dThe Center for Musculoskeletal Research, University of Rochester Medical Center, Rochester, NY 14642, USA.

† Electronic Supplementary Information (ESI) available: Detailed experimental protocols and additional spectroscopic data and microscopic images. See DOI: 10.1039/c000000x/

1. A. R. Hirst, B. Escuder, J. F. Miravet and D. K. Smith, *Angew. Chem., Int. Ed.*, 2008, **47**, 8002-8018.
2. M. C. Branco and J. P. Schneider, *Acta Biomaterialia*, 2009, **5**, 817-831.
3. B. Xu, *Langmuir*, 2009, **25**, 8375-8377.
4. S. I. Stupp, *Nano Letters*, 2010, **10**, 4783-4786.
5. X. Zhao, F. Pan, H. Xu, M. Yaseen, H. Shan, C. A. E. Hauser, S. Zhang and J. R. Lu, *Chem. Soc. Rev.*, 2010, **39**, 3480-3498.
6. Y. Pan, X. Du, F. Zhao and B. Xu, *Chem. Soc. Rev.*, 2012, **41**, 2912-2942.
7. D. M. Ryan and B. L. Nilsson, *Polym. Chem.*, 2012, **3**, 18-33.
8. H. Wang and Z. Yang, *Nanoscale*, 2012, **4**, 5259-5267.
9. L. Haines-Butterick, K. Rajagopal, M. Branco, D. Salick, R. Rughani, M. Pilarz, M. S. Lamm, D. J. Pochan and J. P. Schneider, *Proc. Natl. Acad. Sci.*, 2007, **104**, 7791-7796.
10. J. H. Collier, J. S. Rudra, J. Z. Gasiorowski and J. P. Jung, *Chem. Soc. Rev.*, 2010, **39**, 3413-3424.
11. J. P. Jung, J. Z. Gasiorowski and J. H. Collier, *Biopolymers*, 2010, **94**, 49-59.
12. Z. M. Yang, K. M. Xu, Z. F. Guo, Z. H. Guo and B. Xu, *Adv. Mater.*, 2007, **19**, 3152-3156.
13. J. A. Craig, E. L. Rexeisen, A. Mardilovich, K. Shroff and E. Kokkoli, *Langmuir*, 2008, **24**, 10282-10292.
14. T. Xiao, J. Takagi, B. S. Coller, J.-H. Wang and T. A. Springer, *Nature*, 2004, **432**, 59-67.
15. J.-P. Xiong, T. Stehle, R. Zhang, A. Joachimiak, M. Frech, S. L. Goodman and M. A. Arnaout, *Science*, 2002, **296**, 151-155.
16. M. D. Pierschbacher and E. Ruoslahti, *Nature*, 1984, **309**, 30-33.
17. D. S. W. Benoit and K. S. Anseth, *Biomaterials*, 2005, **26**, 5209-5220.
18. V. Jayawarna, M. Ali, T. A. Jowitt, A. F. Miller, A. Saiani, J. E. Gough and R. V. Ulijn, *Adv. Mater.*, 2006, **18**, 611-614.
19. V. Jayawarna, S. M. Richardson, A. R. Hirst, N. W. Hodson, A. Saiani, J. E. Gough and R. V. Ulijn, *Acta Biomater.*, 2009, **5**, 934-943.
20. G. Cheng, V. Castelletto, R. R. Jones, C. J. Connon and I. W. Hamley, *Soft Matter*, 2011, **7**, 1326-1333.
21. J. Kisiday, M. Jin, B. Kurz, H. Hung, C. Semino, S. Zhang and A. J. Grodzinsky, *Proc. Natl. Acad. of Sci. U. S. A.*, 2002, **99**, 9996-10001.
22. J. Raeburn and D. J. Adams, *Chem. Commun.*, 2015, **51**, 5170-5180.
23. D. M. Ryan, T. M. Doran and B. L. Nilsson, *Langmuir*, 2011, **27**, 11145-11156.
24. D. M. Ryan, T. M. Doran and B. L. Nilsson, *Chem. Commun.*, 2011, **47**, 475-477.
25. D. M. Ryan, T. M. Doran, S. B. Anderson and B. L. Nilsson, *Langmuir*, 2011, **27**, 4029-4039.
26. D. M. Ryan, S. B. Anderson, F. T. Senguen, R. E. Youngman and B. L. Nilsson, *Soft Matter*, 2010, **6**, 475-479.
27. D. M. Ryan, S. B. Anderson and B. L. Nilsson, *Soft Matter*, 2010, **6**, 3220-3231.
28. R. A. Hule, R. P. Nagarkar, A. Altunbas, H. R. Ramay, M. C. Branco, J. P. Schneider and D. J. Pochan, *Faraday Discuss.*, 2008, **139**, 251-264.
29. C. Yan and D. J. Pochan, *Chem. Soc. Rev.*, 2010, **39**, 3528-3540.
30. M. Zhou, A. M. Smith, A. K. Das, N. W. Hodson, R. F. Collins, R. V. Ulijn and J. E. Gough, *Biomaterials*, 2009, **30**, 2523-2530.
31. S. Aidoudi, K. Bujakowska, N. Kieffer and A. Bikfalvi, *PLoS One*, 2008, **3**, 2657.
32. M. A. Horton, *Int. J. Biochem. Cell Biol.*, 1997, **29**, 721-725.
33. Q. Wei, T. L. M. Pohl, A. Seckinger, J. P. Spatz and E. A. Cavalcanti-Adam, *Beilstein J. Org. Chem.*, 2015, **11**, 773-783.